

Thermal Relaxation of Residual Stresses induced by Shot Peening in IN718

J. Hoffmeister 1, V. Schulze 1, A. Wanner 1, R. Hessert 2, G. Koenig 2

1 Institute for Materials Science and Engineering I, University of Karlsruhe, Germany

2 MTU Aero Engines, Munich, Germany

ABSTRACT

Shot peening is often used to improve the fatigue life of turbine components applied at elevated temperatures. Therefore it is very important to know the thermal relaxation of residual stresses.

The objective of this work was to analytically describe thermal relaxation of residual stresses in the Ni-based superalloy IN718 induced by shot peening. Shot peened specimens were aged in a temperature range up to 750°C for aging times between 0.1 and 100 hours. The time dependent changes in the residual stress distribution were determined experimentally using X-ray diffraction. It was observed that the position of the residual stress maximum and the zero crossing remains essentially constant during aging. The evolutions of the surface residual stresses and the maximum residual stresses observed in the depth profile could be successfully described on base of a modified Zener-Wert-Avrami-equation.

Assuming constant depth positions of zero crossing and maximum residual stress, the depth distributions of stress-relaxation can be completely described by a single mathematical function. As a result, two sets of parameters for the surface and maximum residual stresses can be extracted.

Keywords: material modeling, IN718, strain ageing, residual stresses, thermal relaxation

INTRODUCTION

Shot peening can increase significantly the fatigue life of turbine components. The improvement of the properties can be attributed to near-surface residual stresses and work hardening. Because turbine engines work at high temperatures, the positive effects on the mechanical properties may be reduced by the thermal relaxation of residual stresses. For the design of turbines it is therefore very important to know how the stress relaxation is depending on time and temperature.

In this paper the thermal residual stress relaxation occurring in shot-peened samples of the Ni-based superalloy IN718 was investigated in a temperature range up to 750°C and times between 0.1h and 100h. After thermal loading x-ray stress analyses were performed and the experimental results were modeled.

METHODS

The investigations were carried out at age hardened IN718 specimens of size 20x20x5 mm³. One face of the 20x20 mm² areas was shot peened with an Almen intensity of 0,25 mmA.

Each specimen was subjected to a different isothermal heat treatment. Seven different annealing times in the range 0.1 h trough 100 h and five different temperatures less than 750°C. In order to diminish the effects of surface oxidation, the following media were selected for the heat treatments: salt melts for low temperatures, radiation heating for high temperatures and short times and a vacuum furnace for high temperatures and long times.

The surface residual stresses were measured on all specimens before and after the heat treatment by X-ray diffraction on the {311}-interference using Mn-K α -radiation and evaluated using the $\sin^2\psi$ -method applying a Young's modulus of $E^{\{311\}}=200$ GPa, a Poisson's ratio of $\nu^{\{311\}}=0.32$ and a stress-free diffraction angle $2\theta_0^{\{311\}}=151^\circ$. On selected samples the residual stresses depth profiles were measured by stepwise removal of circular surface layers with a diameter of 5 mm via electropolishing and repeated X-ray diffraction measurements unto the zero-crossing of residual stresses. As the electropolished area was small compared to the lateral specimen dimensions and large compared to the depth range covered by the profiling procedure, the effects from stress relaxation could be ignored. All depth profiles were fitted with the following mathematical function using a least-squares-algorithm:

$$\begin{aligned}\sigma^{\text{RS}}(x) &= \sigma_{\text{max}}^{\text{RS}} - (\sigma_{\text{max}}^{\text{RS}} - \sigma_0^{\text{RS}}) \cdot (x - x_{\text{max}})^2 / x_{\text{max}}^2 & \text{for } x \leq x_{\text{max}} \\ \sigma^{\text{RS}}(x) &= \sigma_{\text{max}}^{\text{RS}} \frac{1 - (x - x_{\text{max}})^2 / (x_0 - x_{\text{max}})^2}{\left[1 + (x - x_{\text{max}})^2 / (x_0 - x_{\text{max}})^2\right]^2} & \text{for } x > x_{\text{max}}\end{aligned}\quad (1)$$

The parameters of the function are: σ_0^{RS} for the residual stress at the surface, $\sigma_{\text{max}}^{\text{RS}}$ for the maximal compressive residual stresses, x_{max} for the depth of maximal residual stress and x_0 for the depth of the zero-crossing of the residual stress course (cp. Figure 1).

It is expected that the residual stress relaxation beneath the surface is different from that at the surface (V. Schulze, 1993). Therefore the maximum residual stress beneath the surface was determined experimentally on every other specimen. These specimens were electropolished after the heat treatment to a depth close to the depth at which the maximum residual stress had been observed before the heat treatment.

RESULTS

In Figure 1 the residual stress profile after shot peening is shown. The maximum residual stress is observed at a depth of approximately 60 μm whereas the zero crossing is nearly 230 μm beneath the surface. The curve linking the residual stress data points represents a best-fit of the mathematical function described by equation (1). The diagram shows also the full width at half maximum (FWHM) of the X-ray interference lines, which is affected by the dislocation density and can thus be used as an indicator about work hardening. The FWHM is maximum at the surface and decreases monotonically towards the core of the material. At depths greater than about 125 μm the FWHM is essentially constant and equal to that observed on the non-peened base material.

In Figure 2 the residual stresses $\sigma^{\text{RS}}(t,T)$ a) at the surface and b) in the compressive stress maximum related to their averaged initial values $\sigma^{\text{RS}}(t=0)$ are plotted versus the annealing time. As expected the residual stress relaxation at the surface is completely different compared to that at the stress maximum. For the modeling for depth-resolved relaxation behavior two different parameters are needed. One describes at the situation at the surface a) and one beneath the surface b). In both cases the residual

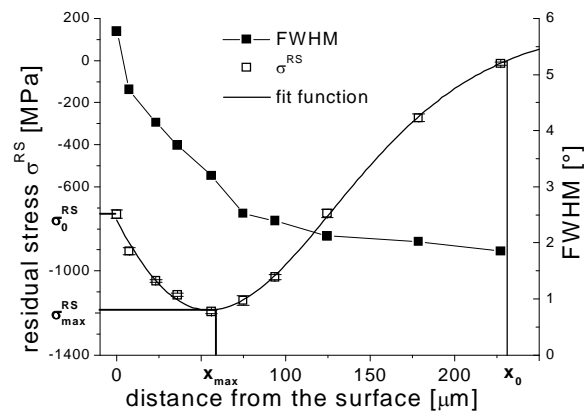


Figure 1: Initial condition after shot peening: the residual stress value and FWHM depth distribution

stresses decrease with increasing time and temperature. An exception is Temperature T3 where the residual stresses decrease only in the first time step until $t=0.1\text{h}$ and afterwards remain nearly constant.

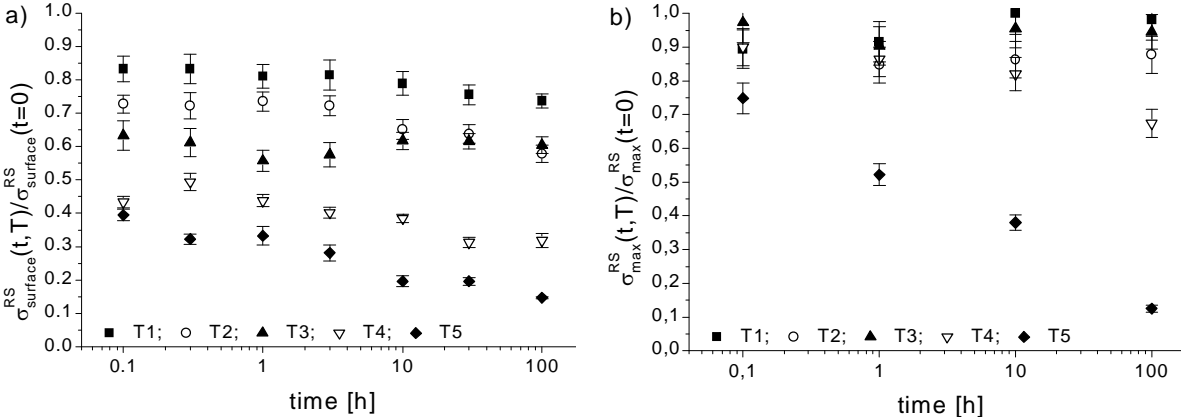


Figure 2: Thermal relaxation of residual stresses: a) at the surface, b) at the compressive stress maximum

In Figure 3a) the residual stress profiles are plotted for selected annealing times and temperatures. The same effect as in Figure 2 can be observed. The residual stresses at the surface relax faster than those beneath the surface. This correlates with the observations by (V. Schulze, 1993) on shot-peened steel and (P.S. Prevey, 1997) on shot-peened IN718. It can also be seen that the locations of the maxima and the zero-crossings of the residual stresses are almost constant. Therefore the depths x_{max} and x_0 in equation (1) are kept constant when fitting this function to the various residual depth profiles measured in this study.

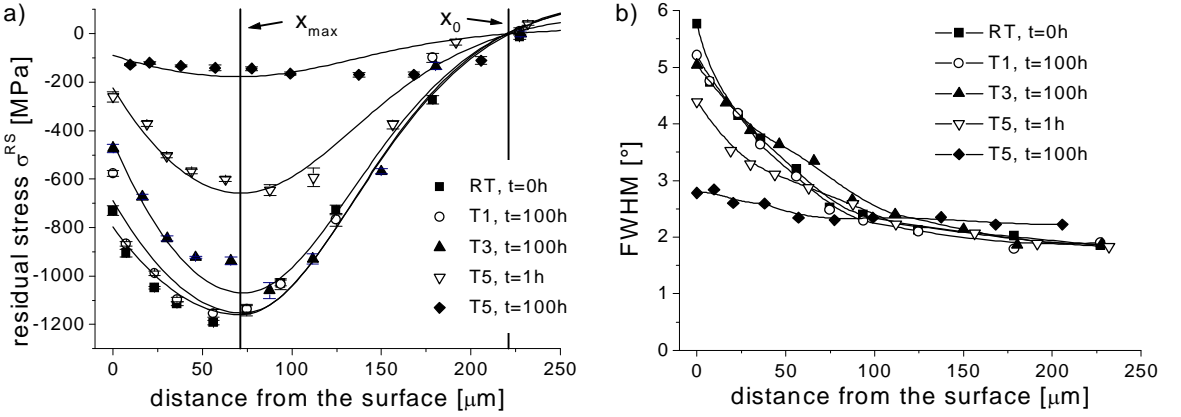


Figure 3: Depth distributions after different heat treatments: a) residual stresses, b) Full width at half maximum (FWHM)

In Figure 3b) the depth distributions of the FWHM are illustrated for the same annealing times and temperatures as in Figure 3a). The macroscopic residual stresses relax much faster than the FWHM or micro residual stresses, respectively. For treatments with $T \leq T3$ and $t \leq 100\text{h}$ barely any relaxation of the FWHM can be observed. The relaxation of FWHM starts at temperatures beyond T3.

MODEL and DISCUSSION

According to (O. Vöhringer, 1983) the isothermal stress relaxation usually can be described by the Zener-Wert-Avrami-approach:

$$\frac{\sigma^{RS}(t,T)}{\sigma^{RS}(t=0)} = \exp\left(-\left(C \cdot t \exp\left(\frac{\Delta H_A}{kT}\right)\right)^m\right) \quad (2)$$

In this approach $\sigma^{RS}(t,T)$ is the magnitude of the residual stress after isothermal annealing for time t at the absolute temperature T , $\sigma^{RS}(t=0)$ is the initial residual stress at room temperature before loading, ΔH_A the activation enthalpy of the rate-controlling process, m an exponent, C a velocity constant and k the Boltzmann constant. Different methods can be used to fit the parameters ΔH_A , m and C of equation (2). In this study the method is described in (J. Hoffmann, 1985) was applied. From equation (2) it follows:

$$\lg\left(\ln\frac{\sigma^{RS}(t=0)}{\sigma^{RS}(t,T)}\right) = \left(m \lg C - \frac{m}{\ln 10} \frac{\Delta H_A}{kT}\right) + m \lg t \quad (3)$$

Thus, by plotting the term shown on the left side of equation (3) against the logarithm of time, straight lines are expected for constant annealing temperatures. The exponent m results from the slopes of these lines and should be independent of temperature. The diagram shown in Figure 4 illustrates that this is not the case. For T3 the experimental results follow a slope near zero, while a slope of about $m = 0,082$ is observed for the four other temperatures.

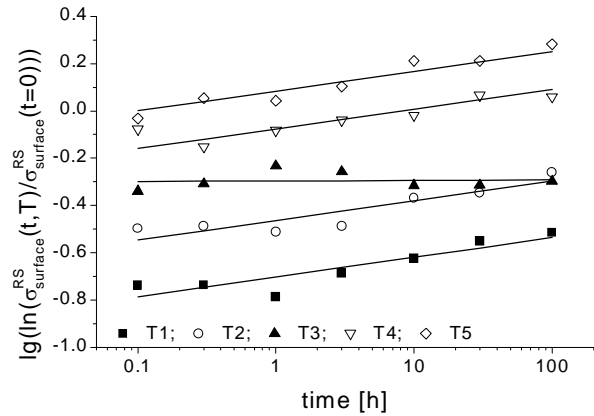


Figure 4: Plot of $\lg(\ln(\sigma^{RS}(t=0)/\sigma^{RS}(t,T)))$ versus time to get exponent m

The activation enthalpy ΔH_A can be derived from the same plots (J. Hoffmann 1985). However, like in the case of m , it is there is no single activation enthalpy ΔH_A which fits to all temperatures covered in our study. The activation enthalpy ΔH_A may be the same for the temperatures T1, T2, T4 and T5 but must be different for T3.

The anomaly observed at temperature T3 requires a modification of equation (2) in such a way that the activation enthalpy ΔH_A and the exponent m become temperature dependent:

$$\frac{\sigma^{RS}(t,T)}{\sigma^{RS}(t=0)} = \exp\left(-\left(C \cdot t \exp\left(\frac{\Delta H_{A1} + \Delta H_{A2} \exp(-(T-T_S)^2/a)}{kT}\right)\right)^{m_1 + m_2 \exp(-(T-T_S)^2/a)}\right) \quad (4)$$

The parameters ΔH_{A1} , ΔH_{A2} rule the magnitude of $\Delta H_A(T)$, as do m_1 and m_2 for $m(T)$ the Equation (2). T_S is the temperature at which the micro-structural process causing the anomaly is dominant. In the present case T_S is equal to T3. The newly introduced parameter a governs the transition between the two different parameter zones. In Figure 5 the influence of a on the temperature dependency of ΔH_A is illustrated. In this case a was set to 1 as the abnormal residual stress relaxation is only observed at temperature T3.

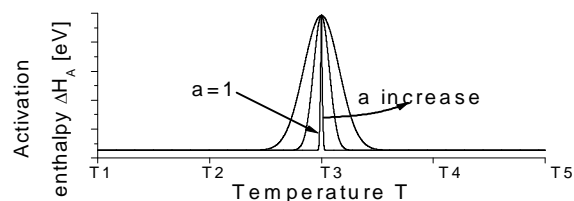


Figure 5: Influence of a on ΔH_A

In Figure 6 the parameter sets of the equation (4) are fitted to the experimental results of Figure 2 using a least-square-algorithm. The results for the surface were $\Delta H_{A1}=2.65$ eV, $\Delta H_{A2}=25.6$ eV, $m_1=0.082$, $m_2=-0.081$ and $C=3.4 \cdot 10^{14}$ 1/h. The calculated mean deviation of the residual stresses in this case is 2.6 %. The calculated activation enthalpy ΔH_{A1} of 2.65eV is close to the value of the activation enthalpy for self-diffusion of Ni in Ni (2.689 up to 3.014eV depending on reference (I. Kaur, 1985)). This implies that the main micro-structural process responsible for the normal residual stress relaxation is achieved by diffusion-controlled creep, which for the given material and microstructure is expected to take place mainly by climbing of edge dislocations. The resulting activation enthalpy at T3 ($\Delta H_{A1} + \Delta H_{A2}=27.25$ eV) is much higher than the activation enthalpy ΔH_{A1} for the other temperatures and implies the existence of another rate-controlling process the exact nature of which is unclear. It can be speculated that the suppression of diffusion-controlled creep in this temperature regime is due to static strain ageing effects (V. Schulze, 2006). Strain aging was already observed in this material and temperature range for example in (M.L. Weaver, 2001).

The best-fit parameters obtained for the data shown in Figure 6b) are $\Delta H_{A1}=3.79$ eV, $\Delta H_{A2}=8.67$ eV, $m_1=0.269$, $m_2=-0.249$ and $C=4.2 \cdot 10^{18}$ 1/h for the maximum compressive stresses. In this case the calculated mean deviation is 6.5 %.

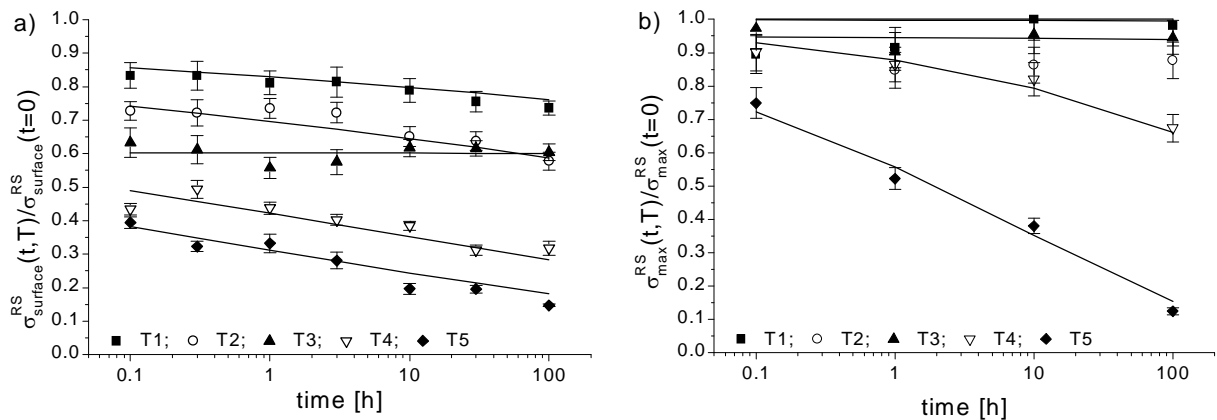


Figure 6: Fitted experimental results: a) surface, b) maximum compressive stress

Assuming that the locations of the maximum residual stresses and the zero-crossing are constant during annealing equations (1) only have the two parameters σ_0^{RS} and σ_{max}^{RS} in order to describe the residual stress depth profile. These two parameters can be calculated with the modified Zener-Wert-Avrami equation (4) for different times and temperatures with the identified parameters for the surface and maximum compressive stresses. The parameters $\sigma_{max}^{RS}(t=0)$ and $\sigma_0^{RS}(t=0)$ are the corresponding initial values measured experimentally. The locations of maximum residual stresses and the zero-crossing could be taken

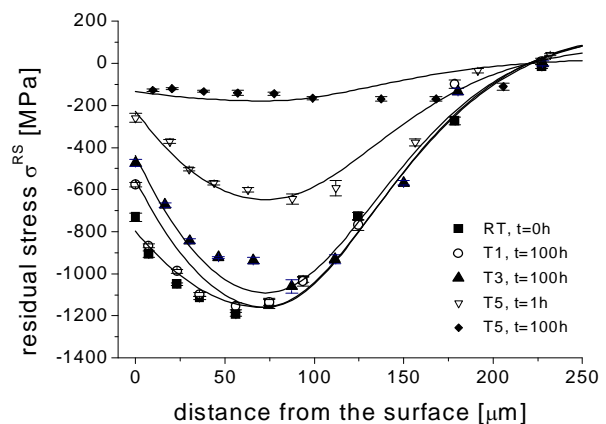


Figure 7: Calculated residual stress depth distributions

from the depth distributions from Figure 3. The result of this procedure is shown in Figure 7. The experimental data and the calculated lines as described above are illustrated. It can be seen that with this enhanced approach it is possible to describe the irregular residual stress relaxation within a wide temperature range.

CONCLUSIONS

The thermal residual stress relaxation of shot peened Ni-base superalloy IN718 was investigated by X-ray diffraction measurements at temperatures up to 750°C and relaxation times between 0.1 h and 100h.

The observed relaxation behaviour showed a distinct anomaly. At an intermediate temperature the stress relaxation was considerably slower than for higher or lower temperatures. This anomaly is supposed to be due to strain ageing effects which suppress the otherwise dominant dislocation creep.

In order to describe thermal relaxation in the whole temperature range a Zener-Wert-Avrami-approach was extended. With this modified equation the experimental results can be fitted well over the whole temperature range.

The depth distributions can be described mathematically assuming constant depths of the maximum residual stresses and the zero-crossings and the predicted surface and maximum residual stress values taken from the extended Zener-Wert-Avrami-approach for the surface and the maximum.

ACKNOWLEDGMENTS

This project is financed by MTU Aero Engines in the frame of LuFo-3 of BMWi.

REFERENCES

Hoffmann, J. (1985), 'Entwicklung schneller röntgenographischer Spannungsmessverfahren und ihre Anwendung bei Untersuchungen zum thermischen Eigenspannungsabbau, PhD thesis, University Karlsruhe (TH)

Kaur I.; Gust W. (1989), 'Handbook of grain and interphase boundary diffusion data', Ziegler Press, Stuttgart, pp.1014-1046

Prevey, P.S.; Hornbach, D.J.; Mason, P.W. (1997), 'Thermal residual stress relaxation and distortion in surface enhanced gas turbine engine components, In: Miliam, D.L.; Poteet Jr., D.A., Pfaffmann, G.D.; Rudnev, V.; Muehlbauer, A.; Albert, W.B. (eds.); 17th ASM Heat Treating Society Conference, ASM, Metals Park, 1997, pp. 3-12

Schulze, V.; Burgahn, F.; Vöhringer, O. et al. (1993), 'Zum thermischen Abbau von Kugelstrahl-Eigenspannungen bei vergütetem 42 CrMo 4, Materialwissenschaften und Werkstofftechnik 24, pp.258-267

Schulze, V. (2006), 'Modern mechanical surface treatment', Wiley-VCH, Weinheim

Vöhringer, O. (1983); 'Abbau von Eigenspannungen', In: Macherauch, E.; Hauk, V. (editor), Eigenspannungen, Messung-Bewertung-Entstehung, Band 1, DGM-Informationsgesellschaft, Oberursel.

Weaver, M.L.; Hale, C.S. (2001), 'Effects of precipitation on serrated yielding in Inconel 718', IN: Loria, E.A; 'Superalloys 718, 625, 706 and Various Derivatives', TMS